Fast turbulent magnetic reconnection and its implications for particle acceleration and high energy emission in compact objects

Giovani H. Vicentin [1]   Grzegorz Kowal [2]   Elisabete de Gouveia Dal Pino [1]   Alex Lazarian [3]

[1]Institute of Astronomy, Geophysics and Atmospheric Sciences . University of São Paulo, Brazil

[2]School of Arts, Sciences and Humanities. University of São Paulo, Brazil

[1]Department of Astronomy. University of Wisconsin - Madison, USA

1. Introduction

Magnetic reconnection is ubiquitous in Astrophysics, from the Earth's magnetotail to the solar and black hole coronae, and becomes an effective mechanism for converting magnetic to kinetic and thermal energy in turbulent environments. We study turbulence's effect on magnetic reconnection rate via high-resolution 3D MHD simulations across an extensive parametric space. With an initial multi-mode perturbation in the system, turbulence is self-generated and sustained in the current sheet, resulting in fast rates of $V_{rec} \sim 0.03 - 0.08$, where $V_A = B/\sqrt{4\pi\rho}$ is the Alfvén velocity. These rates surpass those driven solely by resistive tearing modes/plasmoid instabilities in MHD flows ($V_{rec} \sim 0.01 V_A$). These results align with the theory of turbulent reconnection proposed by Lazarian and Vishniac (1999), where the reconnection rate only depends on the injection scale of the turbulence (ℓ) and its velocity at the injection scale (v_ℓ) as:

$$\frac{V_{rec}}{V_A} = \min\left[\left(\frac{L}{\ell}\right)^{1/2}, \left(\frac{\ell}{L}\right)^{1/2} \right] \left(\frac{v_\ell}{V_A}\right)^2.$$

By injecting thousands of test particles into our turbulent current sheet, we demonstrate that magnetic reconnection is an effective mechanism to accelerate particles to very high energies as a first-order Fermi process, as proposed by de Gouveia Dal Pino and Lazarian (2005), where particles gain energy after each round trip in the current layer, as:

$$\left\langle \frac{\Delta E}{E} \right\rangle \propto \frac{V_{rec}}{c}.$$

2. Methodology and Numerical Setup

We use the AMUN code (Kowal et al. 2009, available at `https://bitbucket.org/amunteam/amun-code`) to solve the isothermal visco-resistive 3D MHD equations. Our three-dimensional domain is a box with $L_x = L_y = 2L_z = 1$, with perfectly conducting, free slipping boundaries along x and y directions, and periodic boundaries along z direction. The initial magnetic field is given by $\mathbf{B} = \hat{z} \times \nabla\psi + B_z \hat{z}$, where

$$\psi = \frac{1}{2\pi} \tanh\left(\frac{y}{\delta}\right) \cos(\pi x) \sin(2\pi y),$$

and $B_z = 0.5$ is the constant guide field, while the density (ρ) is non-uniform in order to maintain the pressure balance (see Fig. 1). We inject a multi-mode perturbation (see Alvelius, 1999, and Kowal et al., 2009) with $k = 128$ from time $t = 0$ up to $0.1\, t_A$. After that, the system evolves without external forcing.
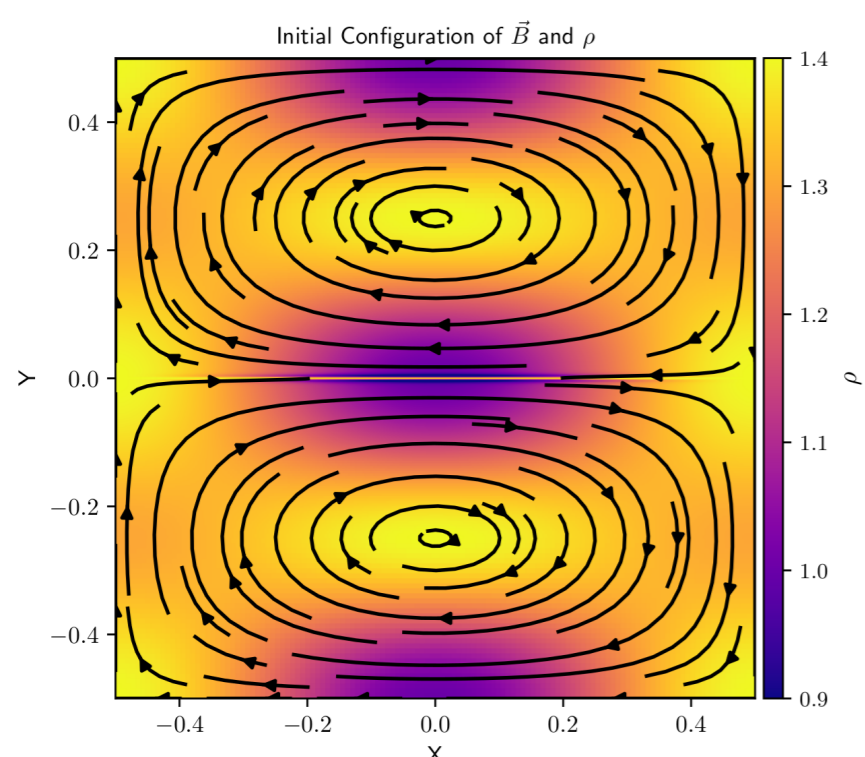
Figure 1. Initial configuration of magnetic field (black arrows) and density (colormap) in the $xy-$plane. The out-of-plane component of the magnetic field (B_z) is set to be constant. Figure from Vicentin et al. (2024).

At each snapshot of the 3D MHD simulations, we inject 10,000 test particles and track their trajectories and the time evolution of their energies using the GACCEL code (Kowal et al. 2012), by solving the equation of motion

$$\frac{d}{dt}(\gamma m \mathbf{u}) = q(\mathbf{E} + \mathbf{u} \times \mathbf{B}),$$

with

$$\mathbf{E} = -\mathbf{v} \times \mathbf{B} + \eta \mathbf{J},$$

where m, q and $\mathbf{u}$ are the particle mass, charge, and velocity, respectively, $\mathbf{B}$ is the magnetic field, $\gamma \equiv (1 - u^2/c^2)^{-1/2}$ is the Lorentz factor, $\mathbf{v}$ is the plasma velocity, $\mathbf{J} = \nabla \times \mathbf{B}$ is the current density, and η is the Ohmic resistivity coefficient.

We normalize our code units to physical units by assuming the magnitude of the magnetic field as $B \approx 1.91$ mG, the Alfvén velocity as $V_A = c/20$, and the Alfvén time being $t_A = 1$ hour, such a way that the unit length is $L = 5.4 \times 10^{10}$ m.

3. Results
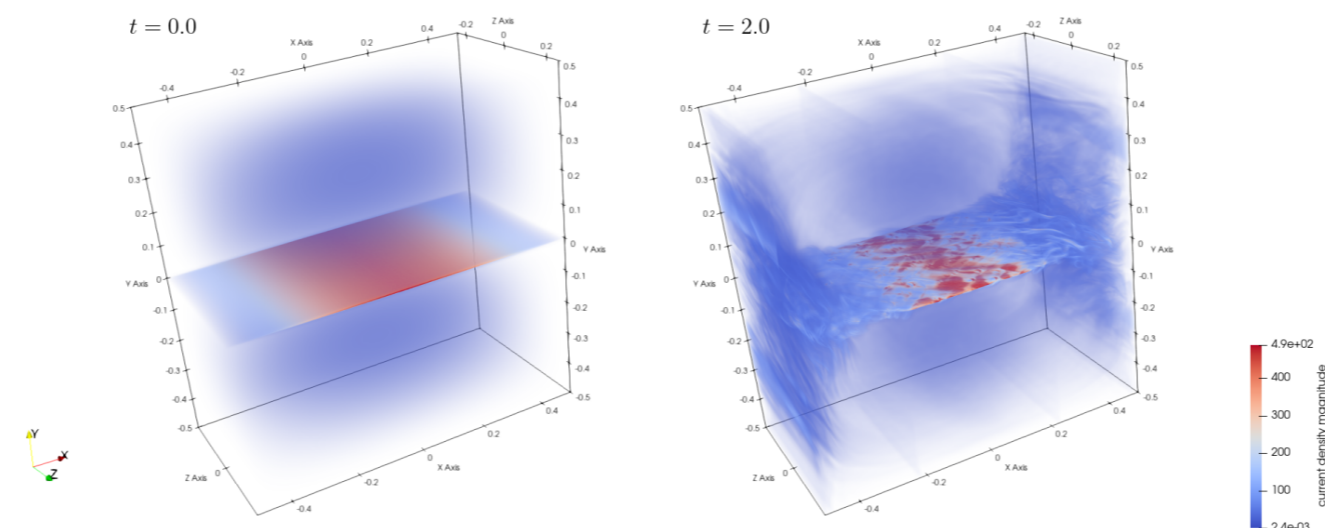
Self-sustained turbulence

Figure 2. 3D visualization of the current density magnitude, $|\mathbf{J}| = |\nabla \times \mathbf{B}|$, at $t = 0$ (left) and $t = 2.0\, t_A$ (right) for the simulation with $S = 10^5$, $Pr_m \equiv \nu/\eta = 1$, and $\beta \equiv p_{th}/p_{mag} = 2.0$. We notice that turbulence is self-sustained in the system even long time after forced injection is stopped. Figure from Vicentin et al. (2024).
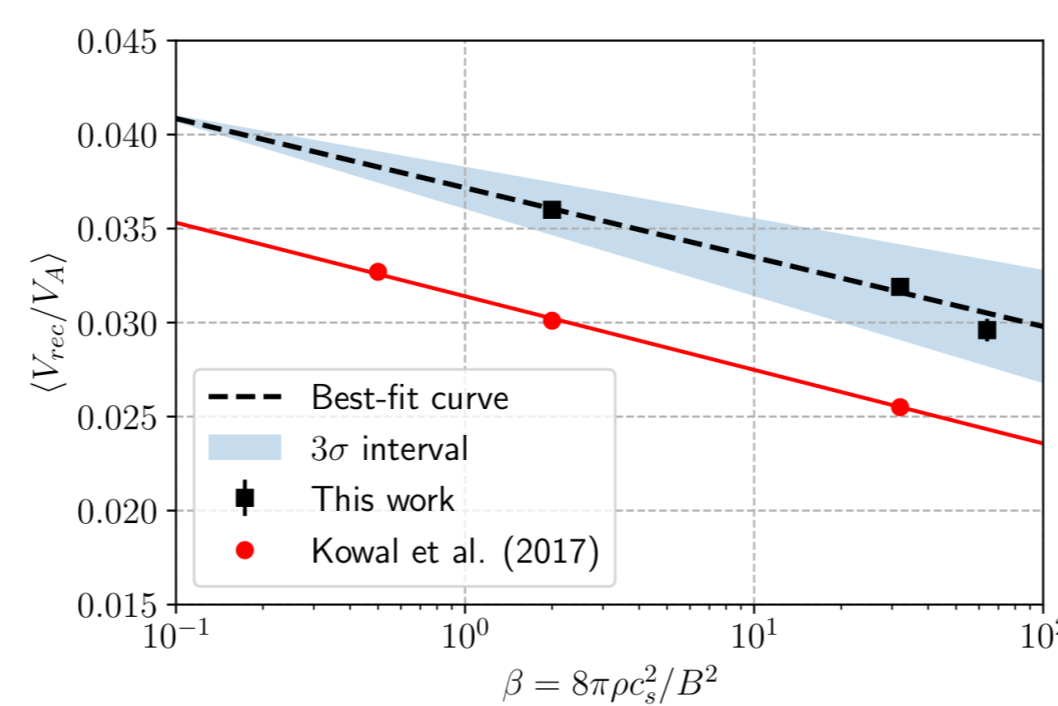
Plasma-β dependence on V_{rec}

Figure 3. Time averaged reconnection rate as a function of plasma$-\beta$. The black dashed line is the best-fit curve, $\langle V_{rec}/V_A = 0.0372 - 0.0016 \log \beta$, for our simulation with $S = 10^5$ and the red dots and line represents the results from self-generated turbulent reconnection performed by Kowal et al. (2017) for $S = 2 \times 10^3$. This result demonstrates the reconnection rate's independence on S, as proposed by Lazarian & Vishniac (1999). Figure from Vicentin et al. (2024).

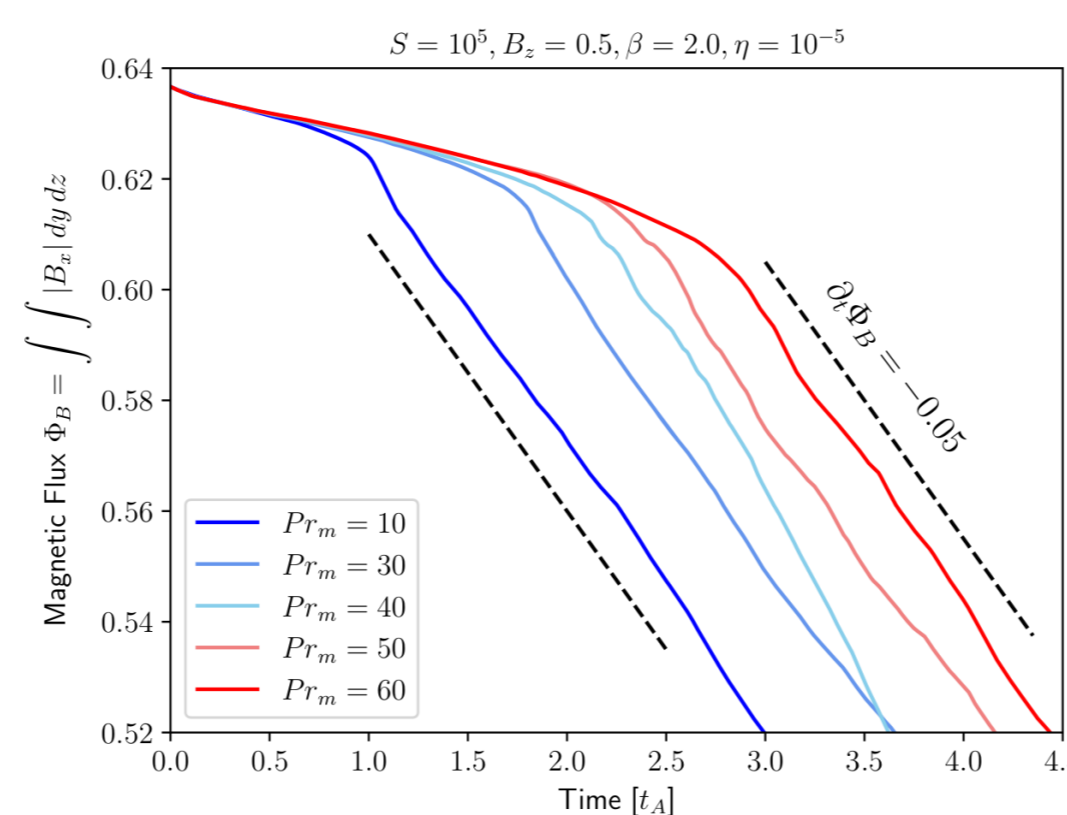### Magnetic Prandtl number (Pr_m) dependence on V_{rec}

Figure 4. Time evolution of the magnetic flux Φ_B for different magnetic Prandtl numbers. The two dashed black lines correspond to a constant reconnection rate of $V_{rec}/V_A = -\partial_t\Phi_B = 0.05$. These rates are compatible with the ones measured in accretion flows and relativistic jets around black holes reported by Kadowaki et al. (2021) and Medina-Torrejon et al. (2021). Figure from Vicentin et al. (2024).
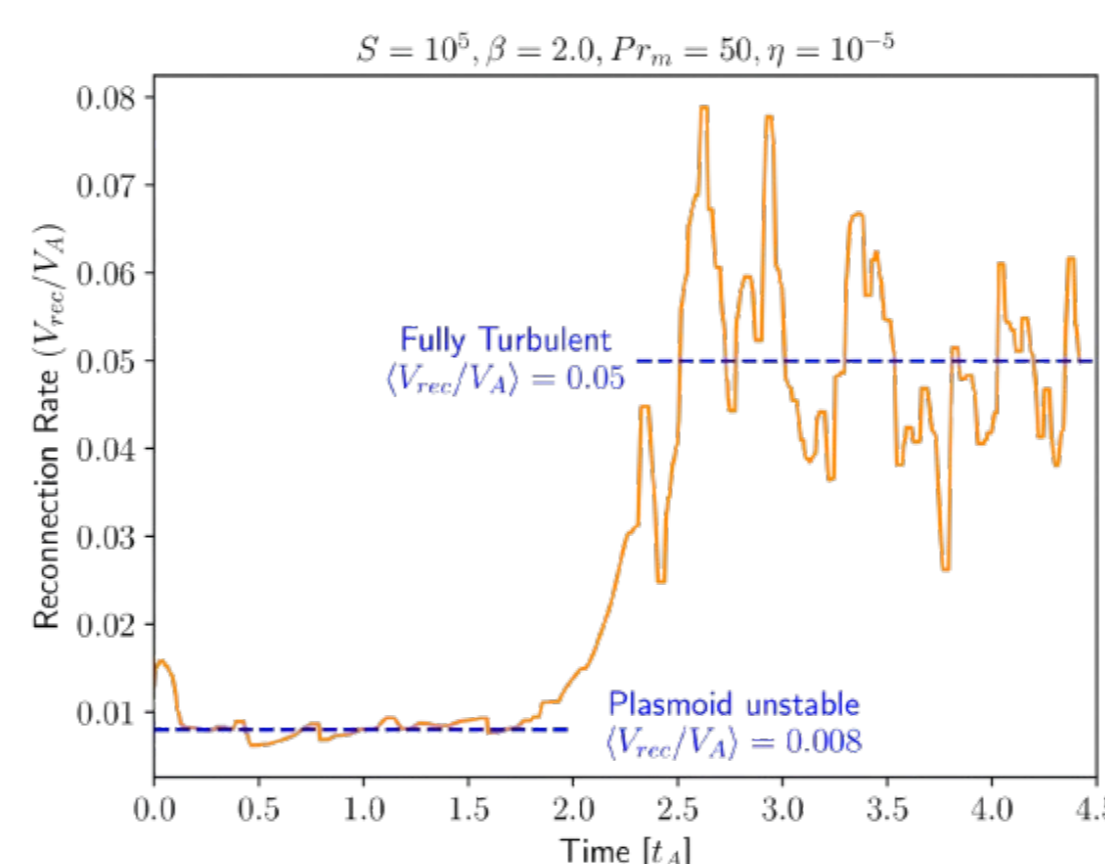
Turbulent VS plasmoid reconnection

Figure 5. Time evolution of the reconnection rate for the simulation with $S = 10^5$, $\beta = 2.0$, and $Pr_m = 50$. The blue dashed lines represent the average reconnection rate of $\langle V_{rec}/V_A \rangle = 0.008$ (tearing mode/ plasmoid unstable regime) and 0.05 (fully turbulent regime). We notice that turbulence enhances the reconnection rate by up to one order of magnitude compared to the rates from tearing mode/plasmoid instability. Figure from Vicentin et al. (2024).
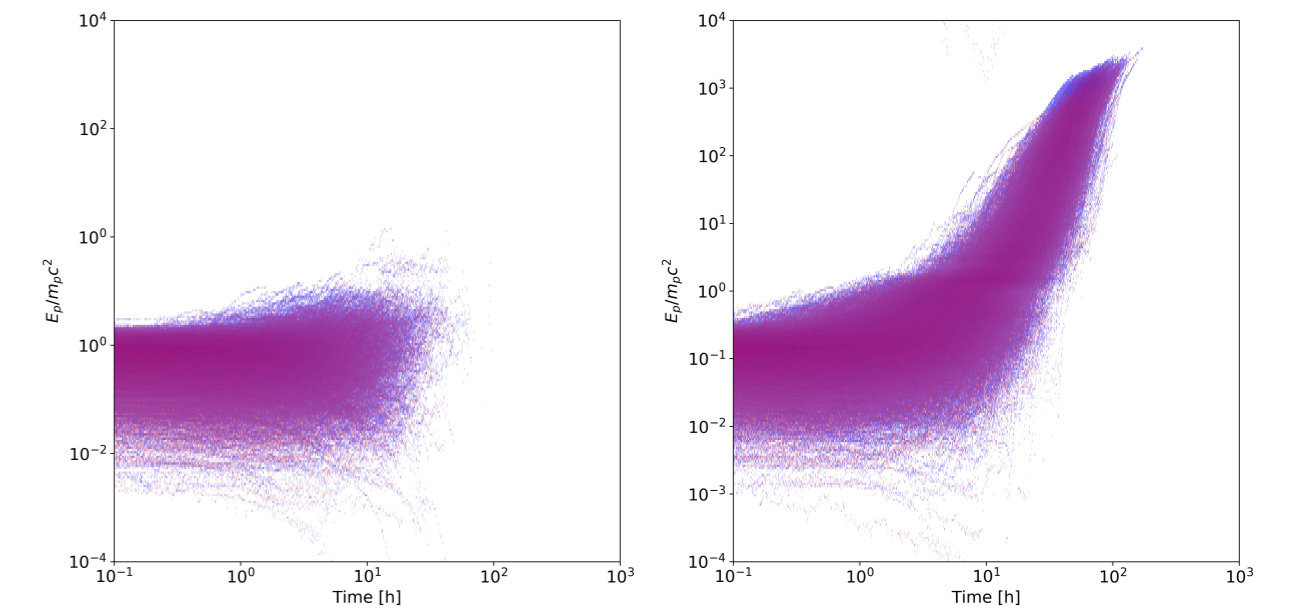
3.1. Particle acceleration

Figure 6. Particle Kinetic energy distribution for 10000 protons accelerated in the plasmoid-unstable (left, at $t = 1.5\, t_A$, $V_{rec} = 0.01$) and in the turbulent (right, at $t = 2.8\, t_A$, $V_{rec} = 0.05$) domains. We notice an exponential energy growth in the turbulent scenario, while particles are not efficiently accelerated in the plasmoid regime. In the turbulent regime, there is a clear transition from an exponential acceleration in time (Fermi regime) to a slower drift regime.
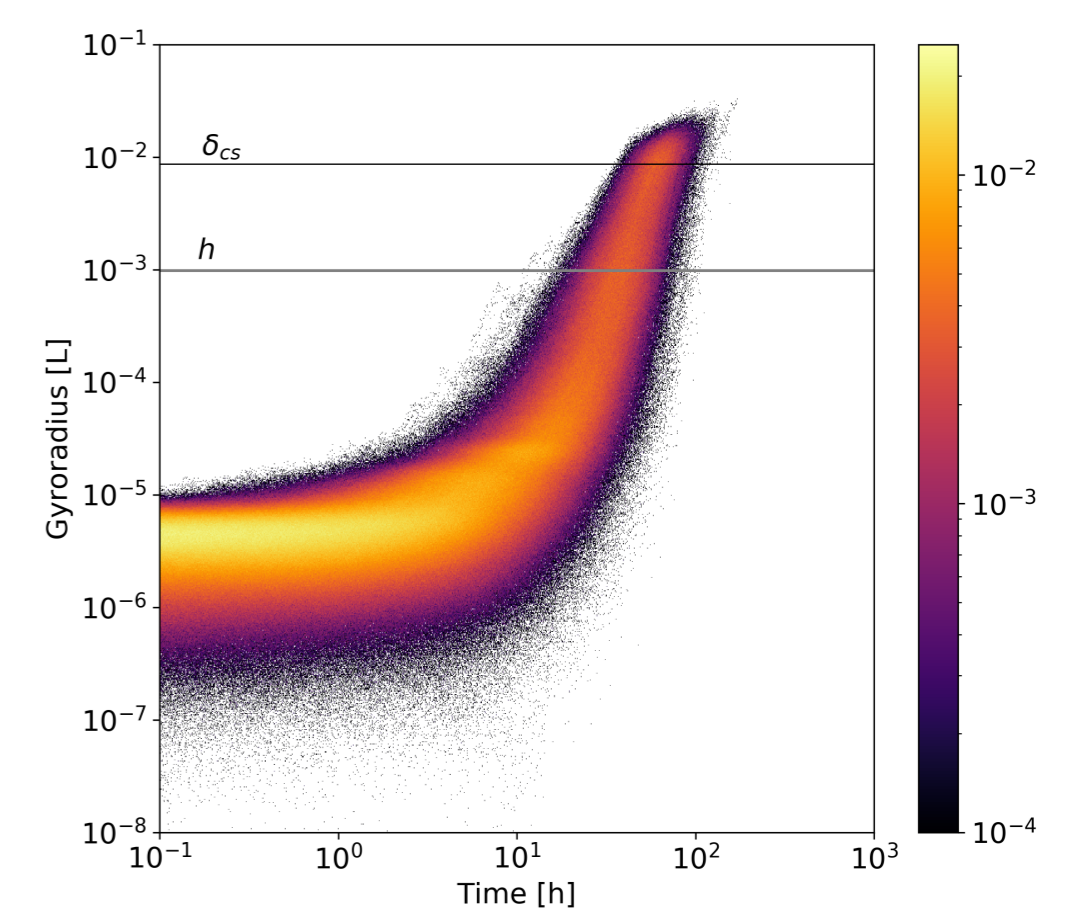
Figure 7. Corresponding Larmor radius distribution for the 10000 protons accelerated in the fast magnetic reconnection turbulent domain at $t = 2.8\, t_A$, for the simulation with $S = 10^5$ and $Pr_m = 50$. We note that the particles change from the exponential (Fermi) acceleration regime to the drift regime, when the Larmor radius exceeds the thickness $\delta \simeq 0.009$ of the reconnection site.

Conclusions

- Turbulence, once initiated, is self-sustained and maintains the reconnection process at enhanced rates;

- There is an inverse dependence of the reconnection rate on the plasma parameter β, which may be related to increasing dissipation of magnetic flux due to supersonic shocks for decreasing β;

- The reconnection rates from our simulations with initially induced turbulence with $S = 10^5$ are of the same order as those obtained in self-generated turbulent models with $S \approx 3 \times 10^3$ (Kowal et al. 2017), demonstrating the independence of V_{rec} on S, as proposed by Lazarian & Vishniac (1999);

- The reconnection rates from our self-sustained turbulent models are systematically larger and grow faster than the ones generated solely by plasmoid instability measured from 2D and 3D MHD simulations. Particles are also efficiently accelerated in the turbulent regime as a first-order Fermi process.

- These findings are fundamental for magnetically dominated astrophysical sources/low-β plasmas, as accretion flows and solar corona, for the acceleration of cosmic rays (e.g., Kowal et al., 2012; Medina-Torrejon et al. 2021, 2023), and the production of non-thermal high energy emission (e.g., de Gouveia Dal Pino and Lazarian, 2005; Khiali et al. 2015, 2016; Rodríguez-Ramírez et al., 2019). See talk by E. de Gouveia Dal Pino.

References

Alvelius, K., 1999, Phys. Fluids, 11, 1880

de Gouveia Dal Pino, E. M. & Lazarian, A. 2005, A&A 441, 845

Kowal, G. et al. 2009, ApJ, 700, 63

Kowal, G. et al. 2012, PRL, 108, 241102

Kowal, G. et al. 2017, ApJ, 838, 91

Lazarian, A. & Vishniac, E. T. 1999, ApJ, 517, 700

Medina-Torrejón, T. E. et al. 2021, ApJ, 908, 193

Vicentin, G. H. et al. 2024, subm. ApJ

Acknowledgements